1998 Annual Air Force Corrosion Program Conference

Analytical Methodology for Assessing Corrosion and Fatigue in Fuselage Lap Joints

Angela Trego, Dale Cope, Patrick Johnson and Doug West
Boeing Information, Space, and Defense Systems (ISDS)

INTRODUCTION

This study investigates the capabilities of two advanced structural analysis codes, a two-dimensional finite element code, FRANC2D/L, and a crack growth analysis code, AFGROW, for estimating corrosion effects on the structural integrity of fuselage lap joints. These analysis tools are shown to predict corrosion effects through two case studies, a test of flat panels with open holes and multiple site damage (MSD) and a test of fabricated lap joint specimens. The first test, conducted by Boeing ISDS, included six 2024-T3 aluminum panels drilled with holes to simulate MSD. The second test, conducted by the National Research Council (NRC) of Canada, performed fatigue tests on fourteen fabricated lap joint specimens that simulated actual aircraft lap joints.

A methodology was developed using the analysis tools to determine the fatigue crack growth life of the coupon specimens. The analysis focuses on determining the effect on predicted life when corrosion damage is modeled, specifically the thinning effect. Analytical results are compared to the experimental results to determine the methodology's effectiveness for estimating corrosion effects on the structural integrity of fuselage lap joints.

ANALYSIS OF FLAT MSD PANELS

The MSD panels were tested at Boeing Product Support Division in Wichita. The test results were investigated for the construction phase of the Corrosion Damage Assessment (CDAF) project under contract with NCI, Inc. and the United States Air Force. Reference 1 provides complete information on panel configuration, testing procedure, and experimental test results for aluminum 2024-T3 and 7075-T6 panels.

The analysis was performed on the 2024-T3 panel, which contained eleven open holes across the width as shown in Figure 1.

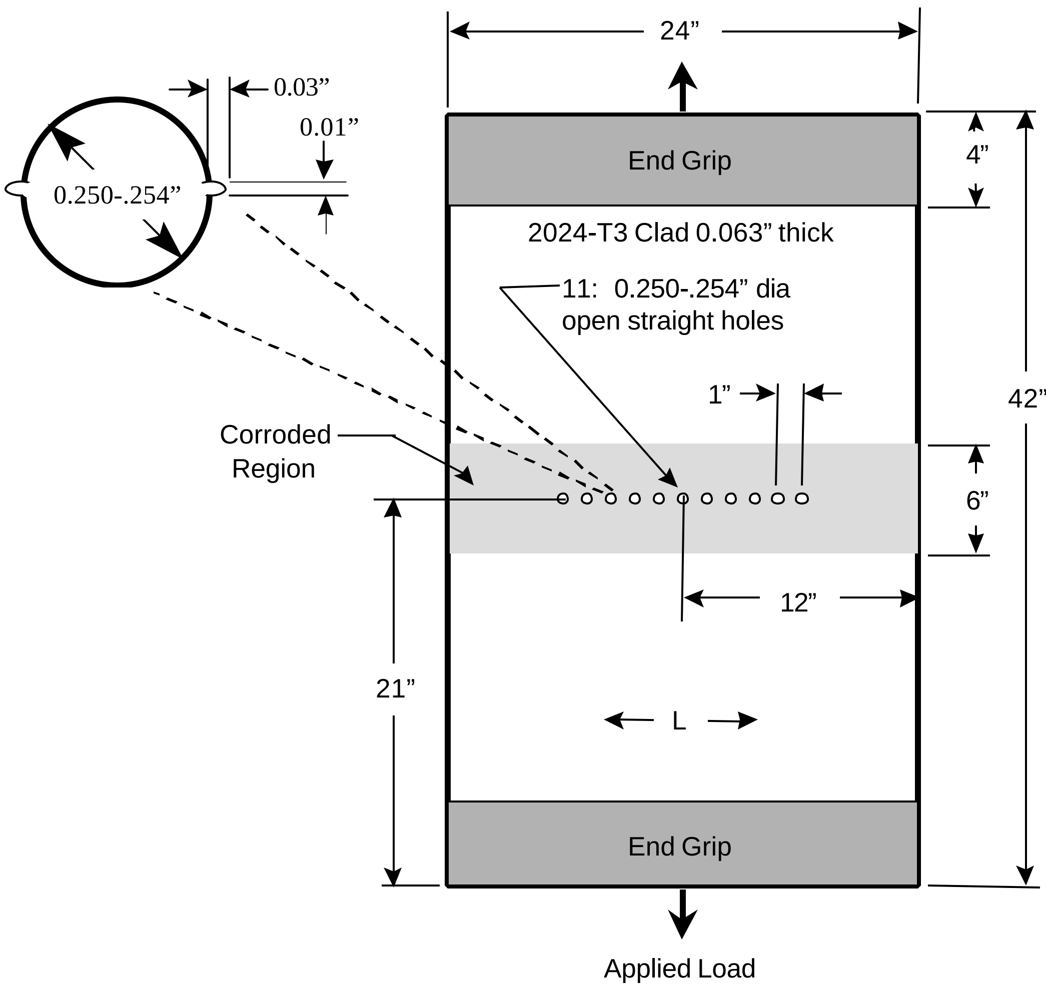

Figure 1. MSD Panel Geometry.

EDM notches were formed at both sides of all eleven holes, introducing starter cracks (see expanded view in Figure 1). A portion of the specimens was exposed to a corrosive environment prior to testing. Severe pitting damage as well as uniform corrosion developed on these panels as a result of the exposure.

Each panel was mechanically cycled under load control conditions. The direction of loading is shown in Figure 1. Tests were performed for the cases defined below.

A. Uncorroded baseline panel fatigued at 10.2 ksi, R = 0.1 - two panels (thickness = 0.062 in.)
B. Corroded panel fatigued at 11.2 ksi, R = 0.1 - one panel (corroded thickness = 0.042 in.)
C. Corroded panel fatigued at 7.6 ksi, R = 0.1 - three panels (corroded thickness = 0.046 in.)

(Above stresses were based on gross area and a nominal panel thickness of 0.062 in.)

Finite Element Models and Analyses

The first step in the analysis of the MSD panels was to perform a stress analysis using a finite element code with crack propagation capability. FRANC2D/L was used for this purpose. Because of symmetry, only half of the panel was modeled. The model consisted of eight-noded plane stress elements. The model geometry, loading and boundary conditions matched those of the experimental test panel (see Figure 1). The EDM notches at the edges of each hole were modeled as simple cracks. Material properties for 2024-T3 clad aluminum were used (see Table 1).

Table 1. Material Properties for 2024-T3 TL Clad Aluminum Used in FRANC2D/L Analyses.

Young's modulus	10.6 msi
Poison's ratio	0.33
Yield strength	40 ksi
Material hardening	Ref. 2
CTOAc	4.5°

The FRANC2D/L model was used to calculate stress intensity factors (SIF's) at each crack tip (eleven tips for the half panel). Based on the resulting SIF values, FRANC2D/L calculated a crack growth increment for each crack, extended each crack, re-meshed around the new crack tips, and then performed another solution on the new mesh. This procedure was performed several times in order to simulate incremental crack growth. SIF data sets were generated as a function of crack length for each crack tip. A single SIF curve was generated based on a best fit curve of the data set.

For the corroded panels, an effective stress was calculated by determining the amount of material loss due to corrosion on the panels and assuming a net section stress increase. The increased stress was then used in subsequent AFGROW crack growth predictions.

It should be noted that, although the FRANC2D/L code is capable of performing rudimentary fatigue crack growth analysis, AFGROW has more sophisticated capabilities in this area, and was therefore selected for this task. The strength of FRANC2D/L is in stress analysis, and the calculation of SIF values for incremental crack growth.

The SIF data can be normalized to be independent of stress, and represented as beta factors. The beta factors may be calculated as:

$$b = \frac{K}{s \cdot \sqrt{p \cdot c}}$$

where K is the stress intensity factor, σ is the far field stress, and c is the crack length. Beta factors were calculated for the average stress intensity factors as a function of crack length. Results are shown in Table 2. These results were used as input for the AFGROW fatigue crack growth analysis.

Table 2. SIF History for MSD Panel.

Average Cracks		
c	**K/s**	**Beta**
0.02	0.639	2.548
0.04	0.770	2.172
0.06	0.829	1.910
0.08	0.870	1.735
0.10	0.911	1.626
0.12	0.960	1.563
0.14	1.016	1.532
0.16	1.078	1.521
0.18	1.146	1.524
0.20	1.218	1.536
0.22	1.295	1.558
0.24	1.385	1.595
0.26	1.495	1.654

Crack Growth Analyses

Next, crack growth analysis was performed using the crack growth code AFGROW. Material properties, geometry, cracking scenario and the spectrum loading are input as program parameters, matching the previously described experimental configuration. The MSD cracks were modeled as a user defined through crack. Note that no retardation models were used in the analysis of the MSD panels since a constant amplitude loading was applied with an R ratio of 0.1.

Figure 2 shows the results from the crack growth analysis. Case A (solid line) represents baseline uncorroded panels fatigued at 10.21 ksi. Case B (dashed line) represents a corroded panel fatigued at a nominal 11.2 ksi. Case C (dash-dot line) represents a corroded panel fatigued at a nominal 7.6 ksi. Test Runs 1 and 2 (data points) correspond to Case A test results. Test Run 4 (data points) correspond to Case B test results. Test Runs 5, 6 and 7 (data points) correspond to Case C test results.

Prediction curves for both the uncorroded (Case A) and corroded (Case B and C) panels appear to be within the scatter of the reported data. Thus, the analytical tools were able to reasonably predict the behavior of the MSD panels.

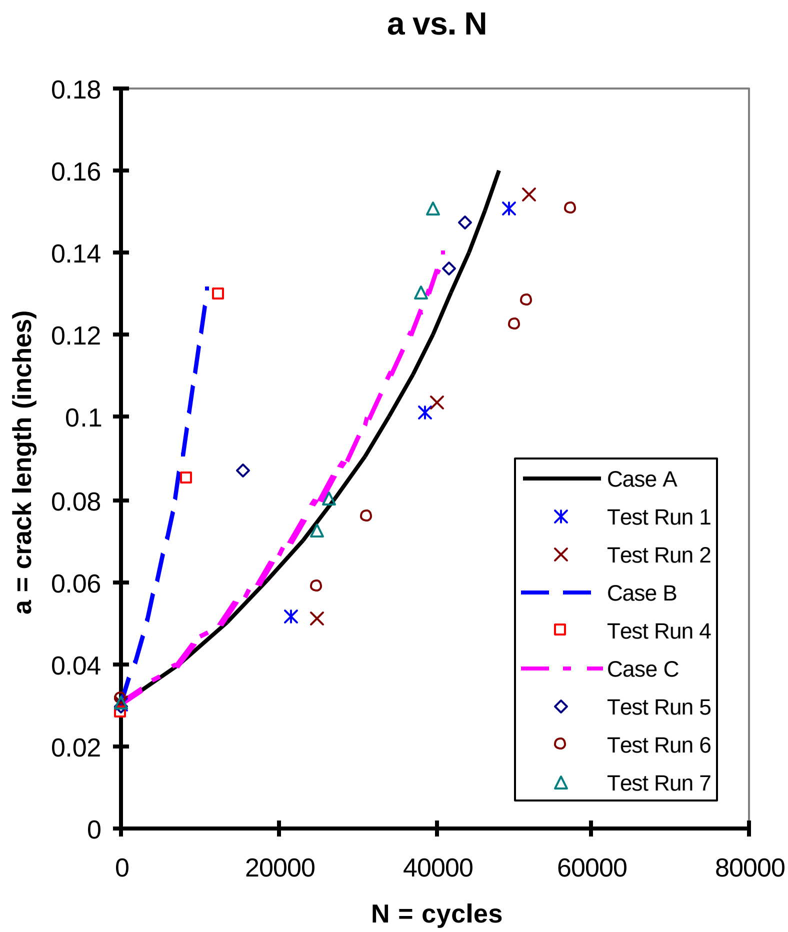

Figure 2. Uncorroded (Case A) and Corroded (Case B and C) MSD Panel Predicted Crack Growth Curves with Test Results.

ANALYSIS OF MSD LAP JOINT SPECIMENS

This section addresses the validation phase of the Corrosion Damage Assessment Framework (CDAF) project. For this phase, riveted lap joint specimens were modeled and analyzed. The lap joint geometry and loading were based on experimental fatigue testing of corroded and uncorroded lap joint specimens conducted by Carleton University and National Research Council (NRC) of Canada. Analysis results were compared to experimental test data.

The lap joint test specimens were constructed of two 0.040 inch sheets of 2024-T3 clad aluminum with three rows of 5/32 inch 2117-T4 rivets. The rivet pattern had a 1.0 inch pitch and row spacing with an edge margin of 0.5. The test specimens were 10 inches wide with 8 fasteners in each row across the width. The experimental study included fatigue testing of nine uncorroded lap joint specimens and five specimens corroded prior to testing. References 3 and 4 discuss in detail the specimen configuration, testing procedure, and the resulting fatigue crack growth data.

Analysis Approach

The analysis of the NRC lap joint paralleled the steps of the MSD panel. A finite element analysis was performed to determine crack tip SIF values and a fatigue crack growth analysis was performed to predict the life of the lap joint. It was observed that 95% or more of the life was exhibited by the lead crack alone. The lead crack occurrences ranged from a single crack on one side of a rivet to a diametric crack with equal length on each side of a rivet. 50% of the occurrences were a single crack, 10% were a diametric crack with equal length, and the remaining 40% were a diametric crack with different lengths on each side of a rivet. As a result, analysis was only performed for the lead crack using two different scenarios. The first scenario consists of a single, radial crack emanating from a single rivet near the center of the specimen. The second scenario consists of a diametric crack emanating from a single rivet near the center of the specimen. From the finite element analysis the SIF's as a function of crack length were generated. Crack growth analysis was then performed to determine the life of the lap joint (crack length versus cycles). These steps were used for specimens with no corrosion and specimens with 2% corrosion.

Finite Element Models and Analyses

Finite element models were created in FRANC2D/L to analyze the lap joint specimen. The model configuration (shown in Figure 3) was based on the geometry, materials, and loading of the experimental specimens. The model consisted of six-noded triangular plate elements. The inner and outer skins, modeled as discrete layers, were attached only at the rivet locations and along the side straps (which were adhesively bonded on the test specimen).

Rivets were modeled using two methods. In the first method, the rivets were modeled as circular plugs in both layers. The plugs were then attached from layer to layer using the adhesive element available in FRANC2D/L. This method was applied to the uppermost row of rivets as indicated in Figure 3, which was shown to be critical in the experimental test results. The second method of modeling rivets used a two-noded spring element. Each node of the element was attached to one of the two skin layers. A single spring element was used for each rivet in the lower two rivet rows. Each spring element was located at the center of the rivet as indicated in Figure 3.

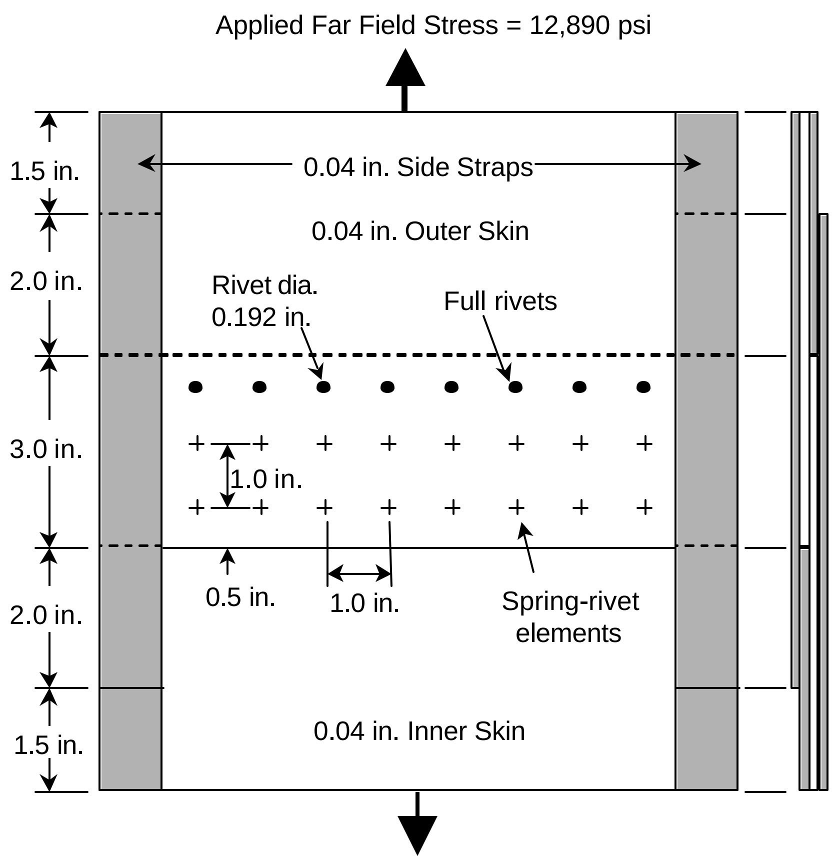

Figure 3. NRC Lap Joint Specimen Configuration.

Contact interface elements were applied to the rivets in the upper row. The contact elements allowed free sliding and opening displacements between the rivet and surrounding skin, but prevented closing displacements. This was accomplished through the standard method of introducing a nonlinear stress-displacement curve, which governed the relative normal displacement between the rivet and skin. A rivet interference was also applied (Reference 5) by adjusting the normal stress-displacement curve to have a positive nonzero value of stress for a zero value of displacement.

Load eccentricity inherent to the single lap joint problem was also considered. An offset between the two skin layers was introduced for this purpose. The offset produces bending in the lap joint. The bending stresses that resulted from this load eccentricity were recorded and agreed well with experimental strain gage data.

While both thinning and pillowing were present, analysis showed that pillowing did not have a significant effect on long crack growth. Therefore, pillowing effects were not included in this analysis.

Cracks were introduced into the upper rivet row according to the two different scenarios. The cracks were incrementally grown using FRANC2D/L's automated crack propagation. The crack tip stress intensity factors (SIF) were recorded at each propagation step. The resulting SIF data are listed in Table 3.

Table 3. SIF History for NRC Lap Joint.

Scenario 1--Single Crack on One Side of Rivet						
Crack	Interference = 0.00075 inch					
Length	*0% Corrosion*			*2% Corrosion*		
c (in)	Kmax	Kres	Beta	Kmax	Kres	Beta
0.05	13730	8377	1.048	13870	8426	1.066
0.10	13740	7429	0.874	13910	7472	0.891
0.15	13480	6422	0.798	13700	6457	0.819
0.20	13800	5861	0.777	14000	5892	0.794
0.25	13960	5336	0.755	14180	5363	0.772
0.30	14550	5082	0.757	14780	5108	0.773
0.35	14950	4849	0.747	15190	4872	0.763
Scenario 2–Diametric Crack with Equal Length at Rivet						
Crack	Interference = 0.00075 inch					
Length	*0% Corrosion*			*2% Corrosion*		
c (in)	Kmax	Kres	Beta	Kmax	Kres	Beta
0.05	13910	8529	1.053	14070	8576	1.075
0.10	14440	7757	0.925	14630	7797	0.946
0.15	14910	6862	0.910	15230	6894	0.942
0.20	16080	6399	0.947	16340	6427	0.970
0.25	16850	5939	0.955	17200	5963	0.984
0.30	18120	5755	0.988	18450	5777	1.013
0.35	19130	5543	1.005	19400	5563	1.024

Crack Growth Analyses

Next, analysis was performed using the crack growth code AFGROW. Inputs include a constant amplitude of 12.89 ksi, an R ratio of 0.02, and 2024–T3 clad aluminum with a da/dn lower limit of 10^{-9}. The crack was modeled as a user defined through crack. Figures 4 and 5 show the results for each predicted scenario (solid lines) versus the lead cracks' test data (data points along dotted lines) for the uncorroded and corroded specimens. The lead cracks' test data is identified in the figures by specimen number and crack location ie., F0-6L is the lead crack on the left side of rivet 6 in the fatigued specimen 0.

Prediction curves for both the uncorroded scenarios 1 and 2 and corroded scenarios 1 and 2 bound the reported data. Thus, the analytical tools were able to reasonably predict the life of the lap joints.

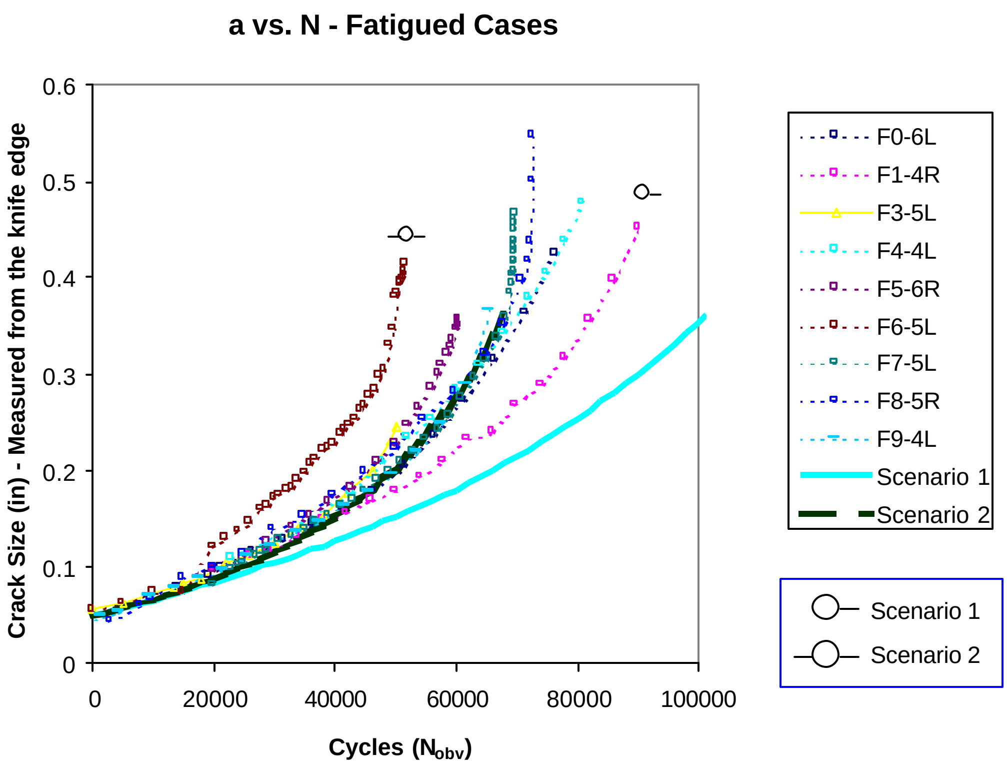

Figure 4. Uncorroded NRC Lap Joint Predicted Crack Growth Curve.

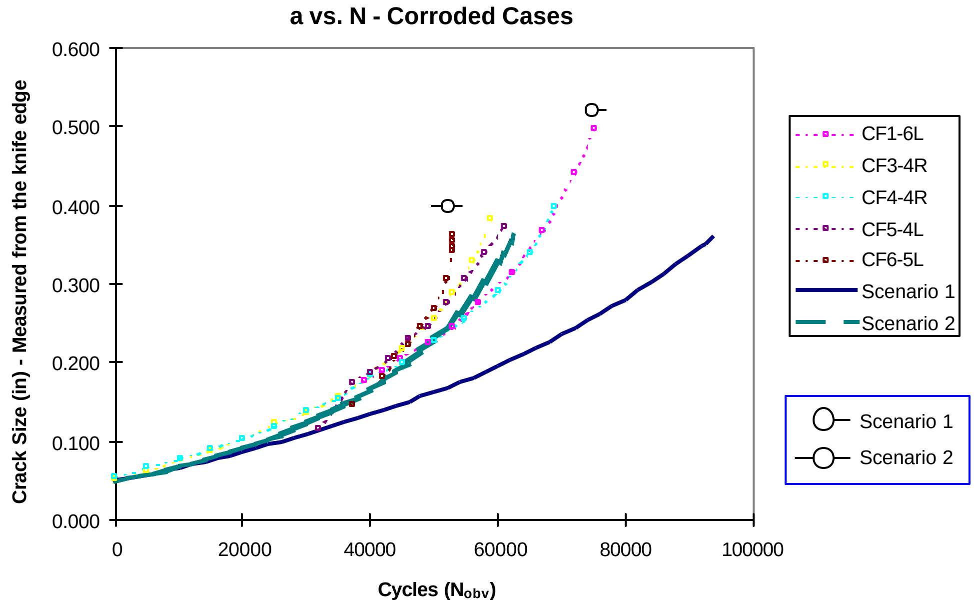

Figure 5. Corroded NRC Lap Joint Predicted Crack Growth Curve.

Conclusions

Results showed good agreement between predicted and experimental life data for the baseline and corroded configurations. Analytical results were compared to the experimental results to determine the methodology's effectiveness for estimating corrosion effects on the structural integrity of fuselage lap joints. A methodology was developed using the analysis tools to determine the fatigue crack growth life of the coupon specimens. These analysis tools were shown to predict corrosion effects through two case studies, a test of flat panels with open holes and multiple site damage and a test of fabricated lap joint specimens.

REFERENCES

1. Luzar, "Pre-corroded Fastener Hole Multiple Site Damage Testing," Final Report, EA 96-135OTH-041, Boeing ISDS Post-Production/Derivative Aircraft Division, December 1997.

2. Newman, Dawicke, Sutton and Bigelow, "A Fracture Criterion for Widespread Cracking in thin-sheet Aluminum Alloys," International Committee on Aeronautical Fatigue, 17th Symposium, Stockholm Sweden, June 9-11, 1993, p 13.

3. Eastaugh, Simpson, Straznicky and Wakeman, "A Special Uniaxial Coupon Test Specimen For The Simulation Of Multiple Site Fatigue Crack Growth And Link-Up In Fuselage Skin Splices," AGARD-CP-568, December 95.

4. Scott, "Corrosion and Multiple Site Damage in Riveted Fuselage Lap Joints," Master's Thesis, Carleton University, March 1997

5. Dawicke, Phillips, Swenson and Gondhalekar, "Crack Growth from Loaded Rivet Holes," Structural Integrity of Aging Airplanes, NASA / FAA, Atlanta, GA, April 1992.

6. Swenson and James, "FRANC2D/L: A Crack Propagation Simulator for Plane Layered Structures, Version 1.4 Users' Guide," Kansas State University, December 1997.

7. Harter, Krishnan and Boyd, "AFGROW User's Manual Version 3.1.1," #WL-TR-97-3053, Wright-Patterson AFB, Ohio, February 1998.